Journal of Renewable Materials

Tech Science Press

DOI: 10.32604/jrm.2022.021694

ARTICLE

Exploration of Waterproofness of Concrete and Alkali-Aggregate Using Hydrophobic Impregnation and Coating

Shun Kang[1], Xun Yuan[1], Changwu Liu[1,*], Yulin Chen[1], Xianliang Zhou[1], Haikuan Wu[2] and Zhiguo Ma[3]

[1]College of Water Resource and Hydropower, Sichuan University, Chengdu, China

[2]School of Emergency Science, Xihua University, Chengdu, China

[3]Sichuan Chuanjiao Road and Bridge Co., Ltd., Guanghan, China

[*]Corresponding Author: Changwu Liu. Email: liuchangwu@scu.edu.cn

Received: 28 January 2022 Accepted: 29 March 2022

ABSTRACT

Part of the tunnel spoil can not be used for concrete due to alkali-aggregate reaction (AAR). Water is an indispensable condition for AAR, so separating the alkali-aggregate from water is of great benefit to controlling the AAR. This paper investigates the modification of concrete and aggregate by hydrophobic impregnation and organic coating and then evaluates their waterproof and mechanical properties by dynamic contact angle (DCA), ultrasonic wave velocity, scanning electron microscope (SEM), nuclear magnetic resonance (NMR), and so on. For waterproofness, hydrophobic impregnation and organic coating can both improve the waterproofness of concrete and aggregate. The organic coating is suitable for aggregate because it wrap aggregate well. And aggregate coated by PVA can improve the interfacial transition zone (ITZ). For mechanical properties, both materials will weaken the strength of the interface. Furthermore, concrete made by aggregate with organic coating shows plastic deformation and has a good correlation with the film thickness, a plastic estimation model based on film thickness is proposed. This paper evaluates the waterproof of concrete and aggregate and finds plastic concrete with good aggregate waterproofness which provides a new idea for the application of alkali-aggregate in seepage control facilities of water conservancy projects.

KEYWORDS

Alkali aggregate; SEM; NMR; PVA

1 Introduction

Engineering such as tunnel excavation will produce a large amount of spoil which is a kind of waste, the stacking of spoil will occupy land, cause environmental pollution [1], and form the source causing landslides [2,3]. Some tunnel spoil cannot be recycled into concrete due to the risk for AAR [4]. AAR refers to the chemical reaction between the alkali active ingredients of the aggregate and the alkali substances in the cement resulting in expansion, cracking or even destruction of the concrete [5]. For the mitigation of alkali-aggregate reaction, many scholars have carried out related research, such as the use of lightweight aggregates [6], the use of mineral admixtures [7], the use of lithium salt-containing admixtures [8] or the incorporation of fiber materials [9]. But some scholars focus the alkali-aggregate reaction on water. Water is very important for the following processes in the alkali-aggregate reaction: (1) Depolymerization and

dissolution of silica; (2) Alkali transport in concrete; (3) Swelling of alkali-silica gel. The current consensus among researchers [10–12] is that the swelling of the gel poses a threat to the integrity of the concrete when the humidity is at a high level only. According to Larive [13], the axial expansion of concrete specimens exceeds 1% only when the relative humidity exceeds 80%. There are two ways to reduce the contact of alkaline active ingredients with water: 1) improve the waterproofness of concrete; 2) improve the waterproofness of aggregates. The use of surface protection systems to improve the water resistance of concrete is a research hotspot [14–17]. Surface protection systems are harmonized by European standards, especially EN 1504-2 [18] which include moisture control (MC) and increasing resistivity (IR), these two are closely related. Both MC and IR can be achieved by hydrophobic impregnation and coating. A widely used hydrophobic impregnating material is silane impregnating agent which has been extensively researched on the protection of concrete [19–22], but its protection on aggregate is very little. As an inexpensive multi-purpose organic compound, polyvinyl alcohol (PVA) also has good waterproofness, there is very little research on it to improve the waterproofness of concrete or aggregates. Based on the obvious influence of humidity on AAR [23], we carry out this investigation. In this paper, super-hydrophobic materials (silane impregnating agent) and organic waterproof coating-PVA are selected for modification. Surface protection systems cannot prevent the infiltration of water caused by the cracking of the concrete [11,24], but modified aggregate can isolate alkaline active ingredients from the water completely. And, as an important component of concrete, the aggregate affects the properties of the interface and the ITZ [25–27], thereby affecting the mechanical properties of the concrete too [28]. As for the modification and research methods of concrete, there are many researches worth learning [29,30].

So, this paper studies the modification of concrete and aggregate by polyvinyl alcohol and silicane impregnant with different concentrations and evaluates the waterproof and mechanical properties of the modified concrete. It found that PVA film with the properity of hydrophilia and waterproofness can improve the waterproofness of concrete and aggregate, and PVA's concentration affect the thickness of the PVA film, the relationship between the two is approximately linear. But the thickness has no obvious effect on the hydrophilicity and waterproofness. Meanwhile, PVA can wrap aggregates well and it has a significant negative effect on interfacial adhesion and friction between aggregate and matrix. However, the concrete using PVA modified aggregate shows plastic deformation. The thicker the coating, the more obvious the plastic deformation. Silane waterproofing agent can increase the waterproofness of aggregate significantly and its concentration has a positive effect. But its aggregate coating is easy to desquamate during the concrete deformation, aggregate modified concrete still shows brittle deformation. Moreover, the adhesion between aggregate and mortar is weak because of the hydrophobicity of the aggregate. This leads to a decrease in the compressive strength of concrete, and there is no obvious correlation between the concentration and the compressive strength. Based on the test, this paper proposes a method for estimating the thickness of organic coatings based on ultrasonic waves and a correlation model for the coating thickness of aggregate and plastic properties of concrete. The main contribution of our work is highlighted below:

- The construction of civil engineering will generate a lot of spoil which is a kind of waste, especially the alkali-active spoil and it can be recycled into concrete aggregate by improving water-proof.
- Investigate the microscopic effects of waterproof alkali-aggregate on concrete.
- Investigate the mechanical mechanism of the concrete with waterproof alkali-aggregate.
- Propose a method to calculate thickness of coating of aggregate based on ultrasonic velocity.
- Propose a calculation model of the coating thickness of aggregate and the plastic properties of concrete.

2 Methods and Materials

Tunnel spoil is slate and rhyolite extracted from Dayukou Tunnel in Leshan City, Sichuan Province, China, it has been adopted to make for concrete. The aggregate grading curve is shown in Fig. 1a). The

aggregate is shown in Fig. 1b). The lithofacies analysis [31] of tunnel spoil is shown in Fig. 1c). The alkali-active mineral accounts for 41.6%, there are alkali-aggregate reaction risks [32] of this tunnel spoil and it cannot be used as aggregate directly. The cement used in this paper is common Portland cement (P·O 42.5). The specimen is the standard cubic piece with a size of 100 × 100 × 100 mm. Film conservation in indoor temperature is selected and the specimen is tested after 28 d.

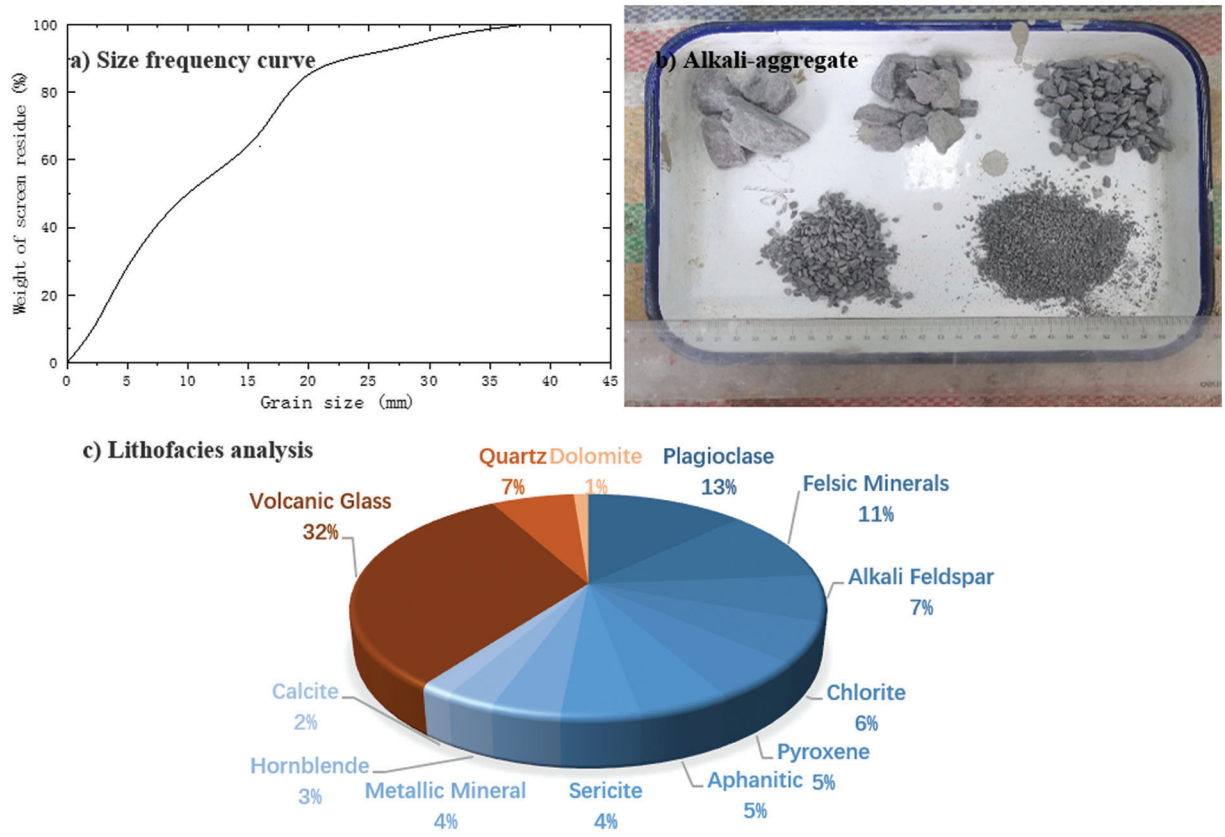

Figure 1: Analysis of tunnel spoil

The technical parameters of waterproof materials are shown in Table 1.

Table 1: Technical parameters of waterproof materials

Silane water repellent	Value	Polyvinyl alcohol	Value
Octyl Triethoxy Silane/%	99.0	Alcoholysis degree/%	99
Hydrolyzable Oxide/(μg·g^{-1})	36	Degree of polymerization	1700
Density/g·ml^{-1}	0.88	–	–

The way of brushing the concrete surface with waterproof materials is called concrete improvement. The way that aggregate is soaked in the waterproof materials for 24 h and then dried naturally is called aggregate soaking. The way that concrete is made by soaked aggregate is called aggregate improvement. The modification schemes of concrete and aggregate are shown in Tables 2 and 3.

Table 2: Concrete modification

Concrete	Water-cement ratio	Method	Object	Materials	Concentration/%
NA				–	0
SS6,26,46		Concrete Improvement	Concrete	silane impregnation agent	6,26,46
PS5,10,15	0.45			PVA	5,10,15
SA6,8,10,12,14		Aggregate Improvement	Concrete	silane impregnation agent	6,8,10,12,14
PA4,6,8,10				PVA	4,6,8,10

Table 3: Aggregate modification

Aggregate	Materials	Concentration/%
N	–	–
S6,8,10,12,14	silane impregnation agent	6,8,10,12,14
P4,6,8,10	PVA	4,6,8,10

3 Result and Discussion

3.1 Waterproofness

The concrete is immersed in water for 7 days and then split and observed, the average immersion depth is about 4.14, 5.06, 4.41, 13.51, 0.97, and 0.65 mm of PS5, PS10, PS15, SS6, SS26, and SS46, respectively. The immersion depth of water for each concentration of PVA is approximately the same, indicating that the variation of concentration has no obvious impact on the immersion depth. Silane impregnation agent has a better effect of anti-immersion than PVA and its effect increases with the increase of concentration. Furthermore, the water absorption rate for 48 h of concrete improvemen and modified aggregate is measured as formula (1), the result is shown in Fig. 2. The test is replicated 3 times.

$$\omega_{wnt} = \frac{m_{2t(s2t)} - m_{1(s1)}}{m_{1(s1)} - m_{3(s3)}} \times 100\% \tag{1}$$

where, ω_{wnt}——Water absorption at different time periods (%)

$m_{1(s1)}$——Total mass of aggregate and tray before drying (g)

$m_{2t(s2t)}$——Total mass of aggregate with Saturated surface dry condition and tray before drying (g)

$m_{3(s3)}$——Mass of tray (g)

t——2 min, 4 min, 8 min, 15 min, 1 h, 2 h, 24 h, and 48 h

The immersion depth and water absorption of concrete have a good consistency. The concrete modified by PVA and silane impregnation agent both reduce the water absorption of concrete in all periods. However, PS5, 10, 15 concrete have no significant difference, and their 48 h water absorption rate is about 44% of the ordinary concrete. The water absorption rate of SS concrete at each period decreases with the increase of the concentration but that of SS26 and SS46 approached the same. Their 48 h water absorption rate is about 30% of the ordinary concrete and is significantly lower than SS6.

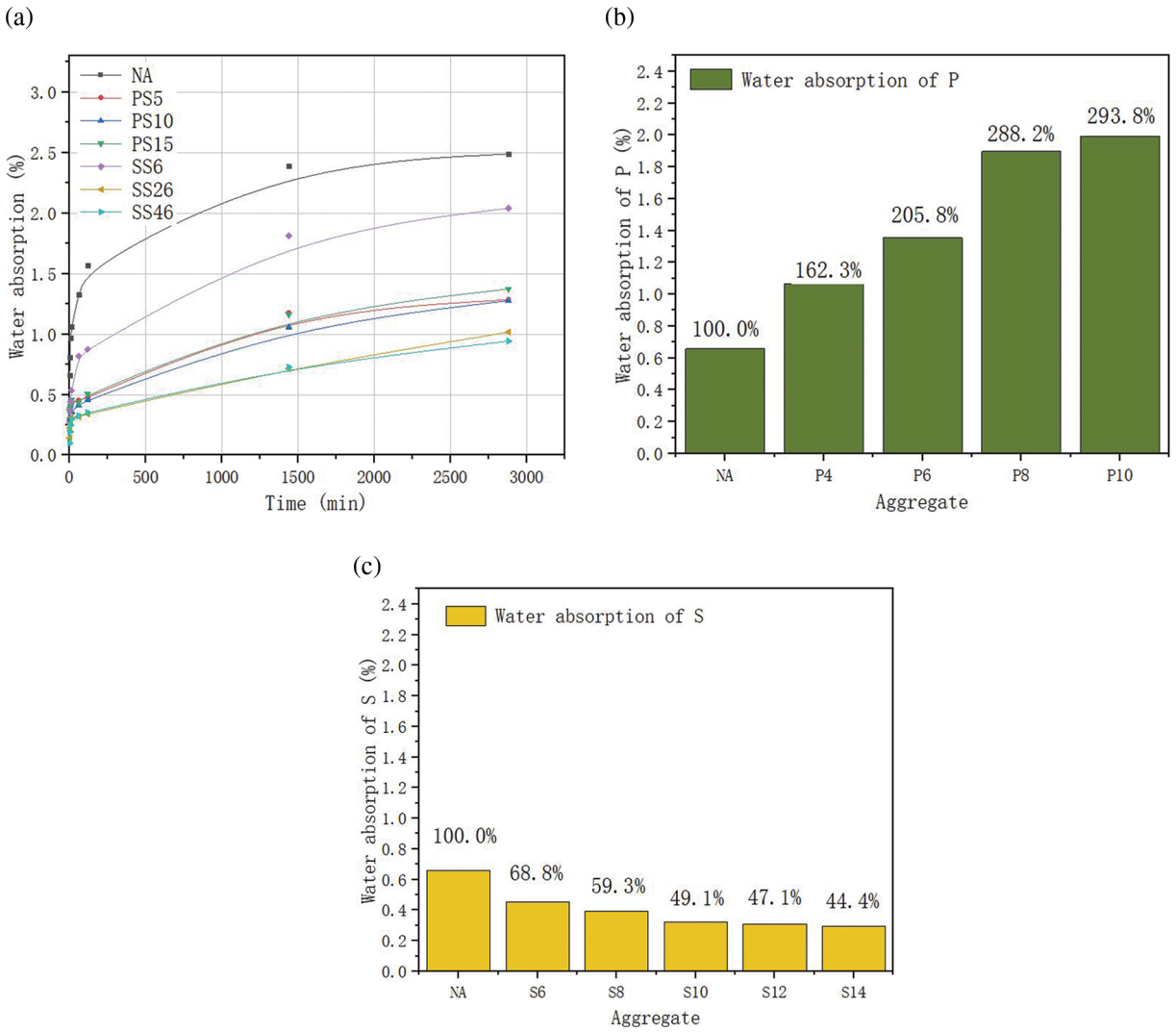

Figure 2: Water absorption of concrete

For aggregates, silane impregnation agent can reduce the water absorption of aggregate. The higher the concentration, the more obvious the effect, it is consistent with the result of the concrete test. For every 2% increase of concentration of silane impregnation agent, water absorption of aggregate decreases by about 6%, and the water absorption of aggregate corresponding to 14% silane is about 44% of the ordinary aggregate. But PVA solution improves the water absorption of the modified aggregate obviously with the increase of the concentration. It is inconsistent with the water absorption of concrete. To research the reasons for the inconsistency of water absorption between aggregate and concrete, a drop of water is dripped on the surface of the modified aggregate, and it is observed by microscope, as shown in Fig. 3.

It can be seen that water can penetrate the N aggregate; the P aggregate shows no strong hydrophobicity but water cannot penetrate it; the S aggregate shows strong hydrophobicity. These properties indicate that PVA and silane impregnation agent can both improve the waterproofness of alkali-aggregate.

The drop hole was fixed, and the dynamic contact angle (DCA) of the PVA film was observed after the distilled water was dropped by the sessile drop method, and its change over time is observed. The contact angle (θ) is the angle from the solid-liquid interface through the inside of the liquid to the gas-liquid

interface. If $\theta < 90°$, the solid surface is hydrophilic, the liquid is easier to wet the solid. The smaller the angle, the better the wettability; if $\theta > 90°$, the solid surface is hydrophobic, the liquid is not easy to wet solids [32]. Two PVA concentrations-low (5%) and high (15%) are selected to test the DCA of the PVA coating by the sessile drop [33]. The variation in contact angle over time is shown in Fig. 4.

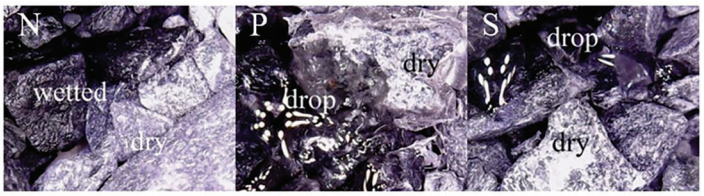

Figure 3: Water absorption of alkali-aggregate

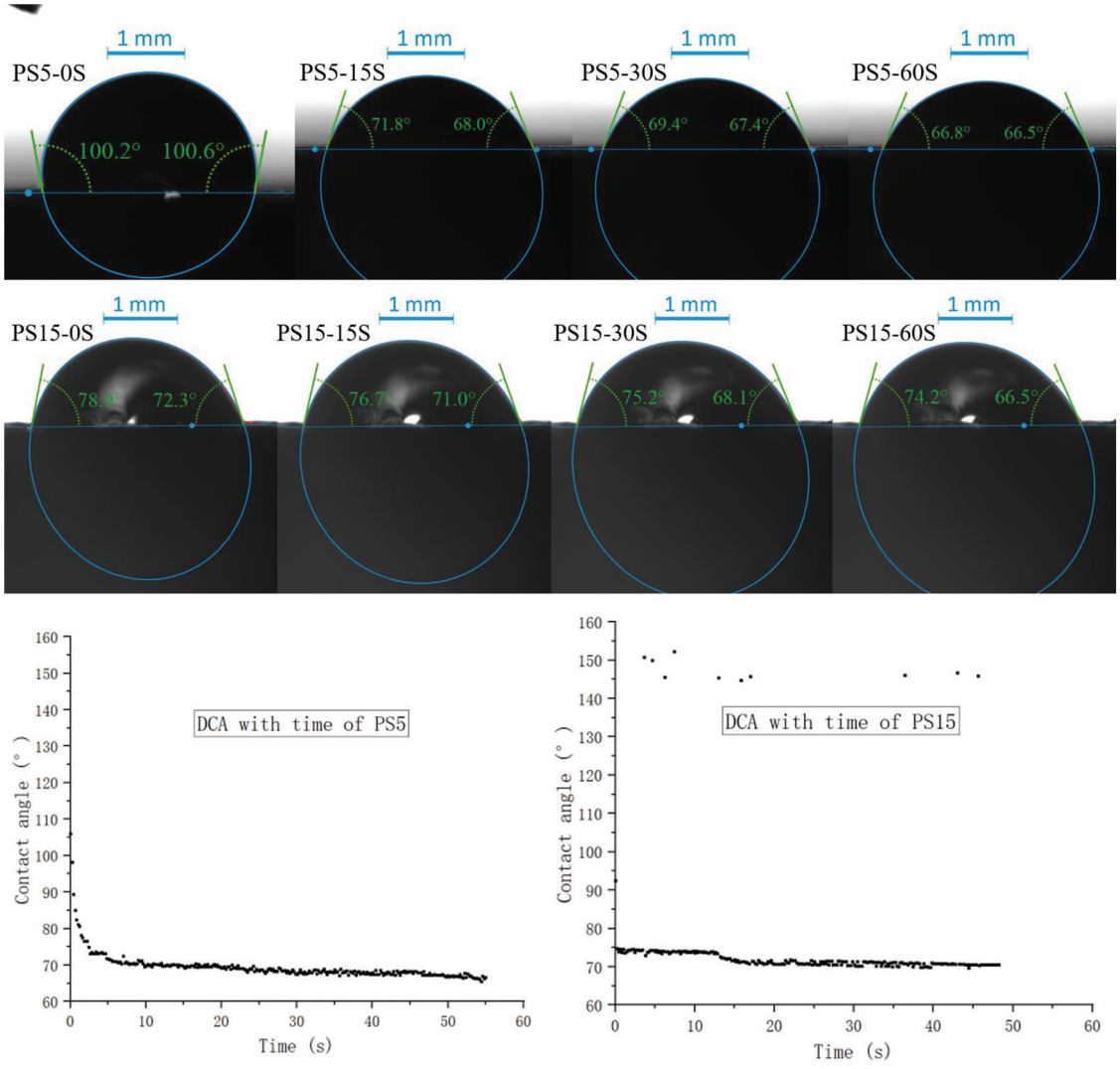

Figure 4: DCA of PS5 and PS15 concrete

The contact angle of the PVA coating is less than 90°, it is hydrophilic which provides the possibility to apply an anti-wear layer outside the PVA film. High concentration (15%) and low concentration (5%) show similar contact angles indicating that the concentration has little effect on the hydrophilic of PVA coating. The contact angle is stable within the 60 s indicating that PVA is a waterproof material. Studies have shown that silane impregnation agent can greatly increase the contact angle of concrete and make the surface of the concrete with hydrophobicity [34,35].

In conclusion, PVA can form an effective waterproof film that can effectively prevent moisture from penetrating concrete and aggregates. The reason for the increase in water absorption after the aggregate is wrapped is that after the PVA forms a film on the surface of the aggregate, it is easy to cause the aggregates to bond to each other. After the aggregate is separated, the surface of the modified aggregate will adhere in excess PVA solids, and the higher the PVA concentration, the more difficult to separate the modified aggregate, and the more PVA solids attached to the aggregates. Since the shape of excess solid is irregular, it is easy to attach a lot of water, so the test showed that the higher the concentration of PVA, the higher the water absorption of the modified aggregates. Water is essential for harmful swelling (ACI SP-144). PVA and silane waterproofing agent can effectively improve the waterproofness of concrete and aggregate.

3.2 Scanning Electron Microscope (SEM)

There are 4 phases in the microstructure of concrete, namely hardened cement paste, aggregate, interface, and the ITZ between the matrix and aggregate [36]. It is helpful to research the performance of concrete by observing the microstructure of each phase of concrete. Research focus on the influence of aggregate modification on aggregate, interface, and ITZ because of the cement and water-cement ratio are the same. The combined part of aggregate and mortar matrix was selected for microscopic observation with scanning electron microscope (SEM). The cylindrical concrete with the size of 50 × 100 mm is tested by GeoSpec 2/150 nuclear magnetic resonance (NMR) core analyzer. The porosity correction needs to be carried out before the test. When the porosity correction error is less than 0.2%, the full water sample is put into the instrument to test. And then LithoMetrix software was used to calculate the permeability of concrete. The result of SEM and NMR of PA and SA concrete is shown in Fig. 5.

For PA-concrete the aggregates and matrix combined well without interstice. For SA-concrete, the aggregates and matrix combined poorly, and there is an interstice at the microscopic. In the concrete making process, PVA can well wrap the aggregate to form a waterproof coating because of its ductility and adhesion [37], and is not easy to break.

For ITZ, Maso [38] described it in detail: First, in the new concrete, a water film is formed around the large aggregates, which causes the water-cement ratio around the aggregates to be higher than the distant parts (the mortar). Then, same as the body of cement paste, the calcium, sulfate, hydroxide, and aluminate ions produced by the decomposition of calcium sulfate and calcium aluminate in the ITZ combine to form ettringite and calcium hydroxide. Due to the high water-cement ratio, the products around these coarse aggregates are coarser crystals, thus forming a skeleton structure with more pores than the cement paste or mortar body.

It can be seen from Fig. 5 that although there are coarse calcium hydroxide (CH) crystals generate in ITZ of PA-concrete, but the ITZ is compact on the micro level. The reason is that the PVA coating is hydrophilic and waterproof (Fig. 4). This will decrease the water-cement ratio around the coated aggregate compare with uncoated aggregate [26,39]. The main reason why the ITZ of SA concrete is not compact on micro level compare with that of PA concret may be that the surface tension caused by the hydrophobicity [40] makes it easy to form a water film on the surface of the modified aggregate. ITZ with lower compactness is often filled with larger crystals. Larger crystals have poor bonding ability, not only because of the weak of van der Waals' force but also because there is the tendency to form a preferred orientation layer [41].

The ITZ is the weak link in the strength chain and is usually regarded as the strength limiting phase.in ordinary concrete [36]. Due to the effects of dry shrinkage, thermal shrinkage and external loads, there is a strain difference between the matrix and the aggregate, and the ITZ is prone to cracking at this time [42]. Subsequently, the micro-cracks develop and coalesce with each other, increasing the permeability of the system. In summary, ITZ with a large water-cement ratio will deteriorate the impermeability and strength of concrete.

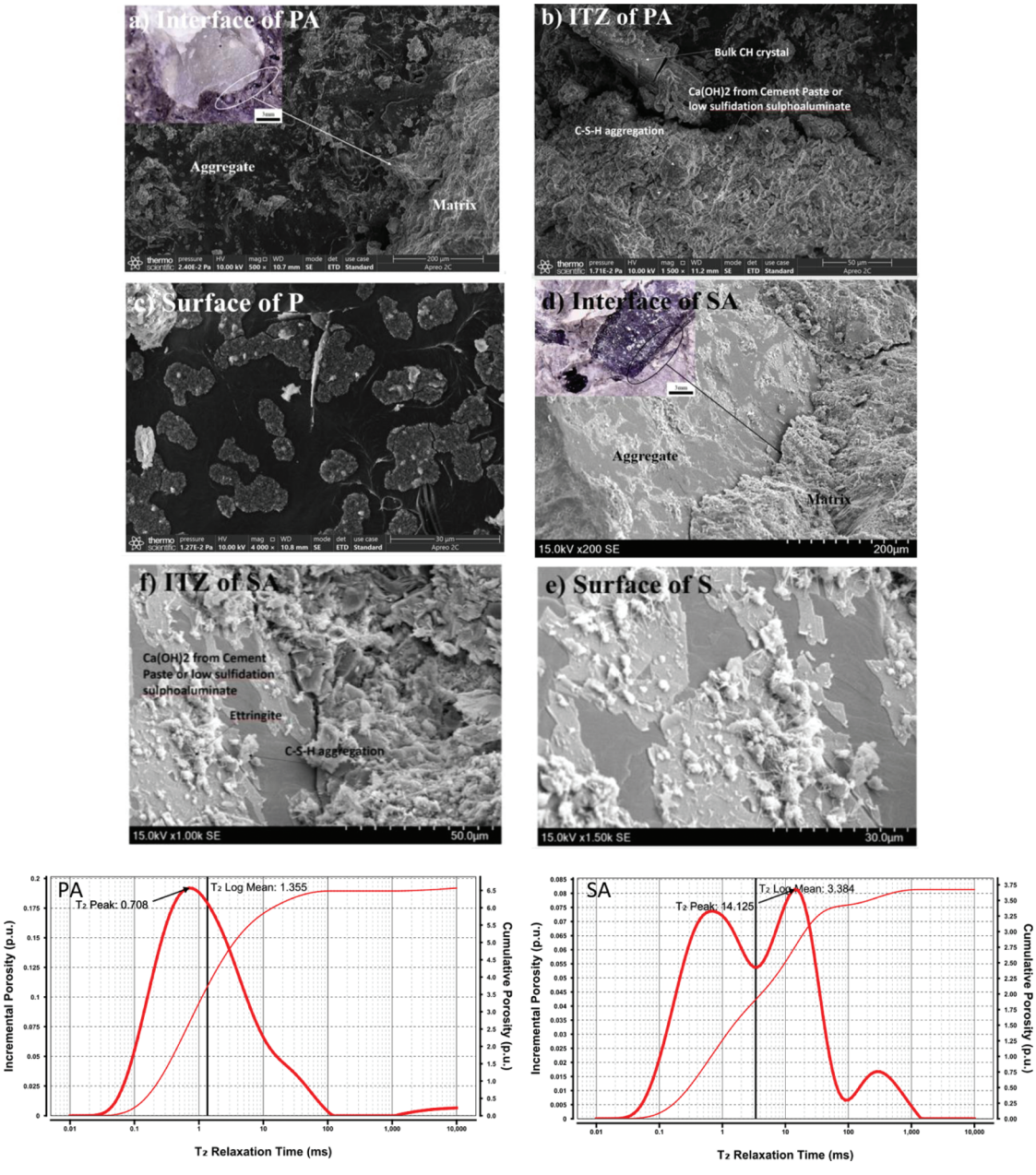

Figure 5: Micro-analysis of PA and SA concrete

For NMR of PA and SA concrete, the permeability coefficient- K(mD) is estimated through the NMR T_2 test results based on the Coates and SDR models, the result is shown in Table 4, where, $\varnothing$ is porosity, %; *FFI* is free fluid porosity, %; *BVI* is bound water porosity, %; T_{2GM} is geometric mean of T_2 distribution mD/(ms2p.u.4); C is coefficient; a is 4; b is 2. From the T_2 spectrum of Fig. 5, the T_2 spectrum of PA concrete has only one peak, and the relaxation time is in the range of 0.1–1 ms indicating that PA concrete has only one pore size, it corresponds to the gel pores in the concrete matrix. The T_2 spectrum of SA concrete has 3 peaks, and the relaxation times are in the range of 0.1∼1 ms, 10∼100 ms and 100∼1000 ms respectively indicating that SA concrete not only has gel pores, but also larger pores formed by the decrease of ITZ compactness. These are consistent with the SEM observations.

Table 4: Permeability coefficient based on NMR

Estimation method	Calculation model	Concrete	Permeability coefficient/mD
Coates with Cut-off	$K = \left(\frac{\varnothing}{C}\right)^a \left(\frac{FFI}{BVI}\right)^b$	PA	0.0024
		SA	1.216e-4
Coates with Spectral Cut-off	$K = \left(\frac{\varnothing}{C}\right)^a \left(\frac{FFI}{sBVI}\right)^b$	PA	0.0222
		SA	0.0018
Log Mean	$K = C\varnothing^a T_{2GM}^b$	PA	1.5542e-4
		SA	6.7687e-6

3.3 Mechanical Mechanism

PVA will form a film on the surface of the concrete, as shown in Fig. 6.

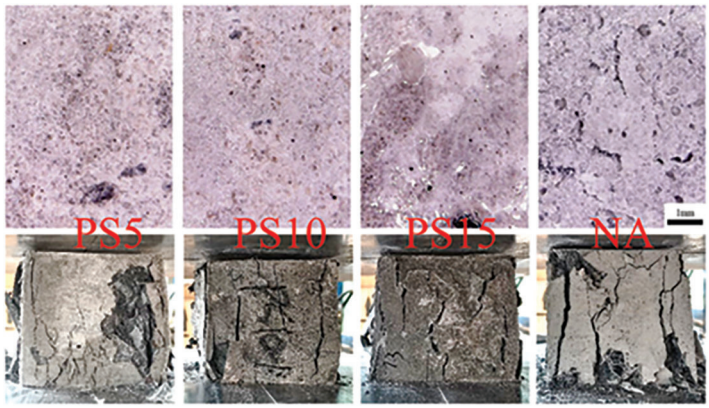

Figure 6: PVA film on the concrete

It is observed by optical microscope that the greater the PVA concentration, the more obvious the surface gloss of the concrete. The reason is that the concentration increases, the thicker the film is. This is verified by the failure of PS concrete also: With the concentration increases, the less fragment drop and the dilatancy of PS concrete is more obvious. The reason is that due to the end effect [43], the largest lateral displacement occurs in the middle part of the specimen, and the lateral displacement is restricted by the PVA film, forming dilatancy. To research the influence of PVA film on the mechanical properties of the surface of concrete, a rebound hammer is used to test rebound values of PS-concrete. And the values of NA, PS5, PS10, and PS15 are about 39.18, 40.01, 39.01, and 38.89, respectively. There is no significant difference in the rebound values of PS-concrete with different concentrations indicating that PVA film does not affect the hardness of the surface of the concrete [44].

The ultrasonic pulse rate method is a commonly used non-destructive testing method that has the characteristics of high detection sensitivity, it is sensitive to concrete density and uneven components [44]. The ZT801 rock mass parameter measuring instrument was used to measure the ultrasonic velocity of the concrete with the 4 flat surface of the specimen as the test point, then take the average, sampling period is 0.2 us. The bond strength of the interface can be characterized by point load strength [45]. We use a point load instrument to explore the influence of the modified aggregate on bond strength. For each concrete specimen, we take about 10 fragments with a diameter of about 6 cm containing the interface and measure the point load strength of the interface. After removing the maximum and minimum values, the average value is taken as the interface bonding strength; Compressive strength is one of the most important performances of concrete. The uniaxial compressive strength test is carried out with a loading rate of 4k N/s. Each test is replicated 3 times. The ultrasonic velocity, load point strength and compressive strength of aggregate-improvement concrete is shown in Fig. 7.

For ultrasonic velocity, the ultrasonic velocity of both SA and PA concrete will decrease with the increase of concentration, and it decrease by about 3.7% and 0.5% of PA and SA concrete for every 2% increase of the concentration. The main reason for the ultrasonic variation of concrete is the influence of ITZ and modified aggregate. It is known from Chapter 3.1 that different PVA concentrations have similar hydrophilicity, so the difference of ITZ on the ultrasonic velocity can be ignored. The main reason that affects the ultrasonic velocity is the thickness of the PVA film covering the aggregate. The greater the concentration, the thicker the film, and the lower the ultrasonic velocity, this is consistent with the observation results for the surface of modified concrete by optical microscope. Due to the hydrophobicity of the surface of the aggregate after silane-modified, the influence of the water film is ignored. The main reason why the ultrasonic velocity of SA-concrete decreases with the increase of the concentration may also be that the thickness of silane impregnation agent film increases with the increase of the concentration, but because the film is extremely thin, the increase in thickness is also very weak, so the decrease of the ultrasonic velocity of SA is very small compared with PA.

Bond strength of the interface of PA-concrete decreases with the increase of concentration, it decreases by about 14.5% for every 2% increase of concentration. Combining microscopic and ultrasonic, it is known that the main factor affecting the adhesion of the interface of PA-concrete is the thickness of the PVA film. The thicker the film, the weaker the adhesion. But bond strength of the interface of SA concrete has no obvious variation with the change of concentration, it is proximately 54.0% of the bond strength of NA concrete. The reason is that due to the hydrophobicity of the silane film, the aggregate and the liquid mortar cannot combine well, resulting in weak adhesion.

The uniaxial compressive strength of PA-concrete decreases with the increase of the concentration and the relationship curve is concave. The compressive strength of the PA-concrete decreases by about 10% for every 2% increase of concentration. The compressive strength of SA-concrete is lower than the control specimen but there is little difference with the change of concentration, it is approximately 77.5% of NA concrete in the concentration range of 6% to 14%. The influence of the matrix on strength of concrete is ignored under the same water-cement ratio and the strength of most aggregates plays a very small role [46], so the destruction of concrete depends on the other 2 phases-interface and ITZ. The interface and ITZ are the weakest links in the strength chain. Referring Mohr-Coulomb theory [47], the main factors affecting the strength of the interface are the interfacial bonding strength and interfacial friction. From the result, the unconfined compressive strength and interfacial bonding strength of PA-concrete show good consistency. The thicker the PVA film, the lower the concrete strength. The reason for the decrease is that the PVA film not only reduces the interfacial bonding strength but also the film has a certain lubricating effect and reduces friction [37]. The unconfined compressive strength and interfacial bonding strength of SA-concrete show good consistency, and both are lower than NA-concrete. The reason is that the hydrophobicity reduces the bonding strength, thereby reducing the compressive strength.

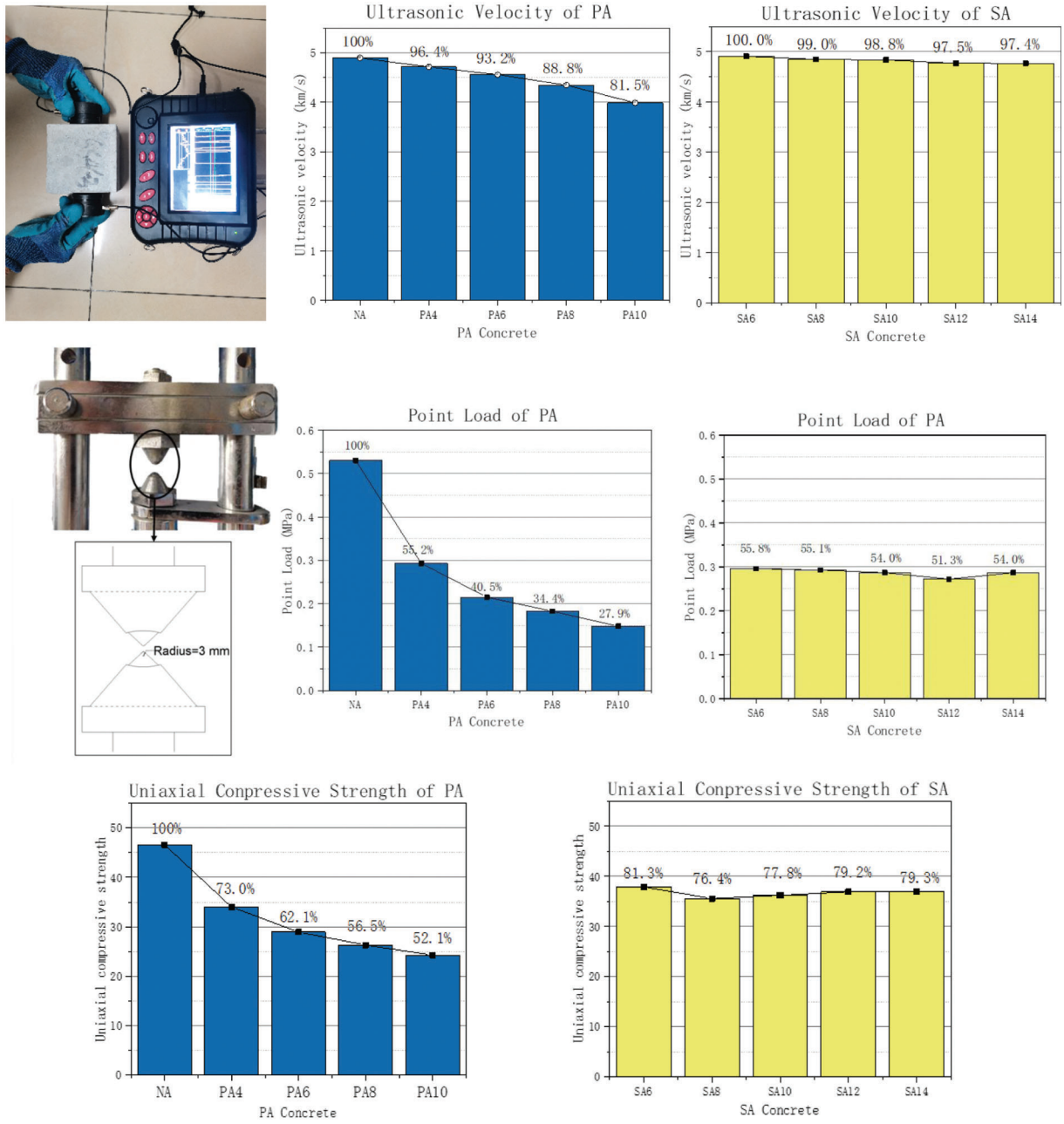

Figure 7: Mechanical analysis of PA and SA concrete

Ignoring the refraction effect of sound through the different media, the thickness of coating of aggregate based on ultrasonic velocity can be calculated according to the following. The overall thickness of the film inside the concrete that has an effect on the ultrasonic velocity is defined as the equivalent film thickness. Assuming that the aggregates are all standard spheres, the thickness of the surface of the concrete that the ultrasonic actually through is defined as the inductive film thickness, as shown in Fig. 8.

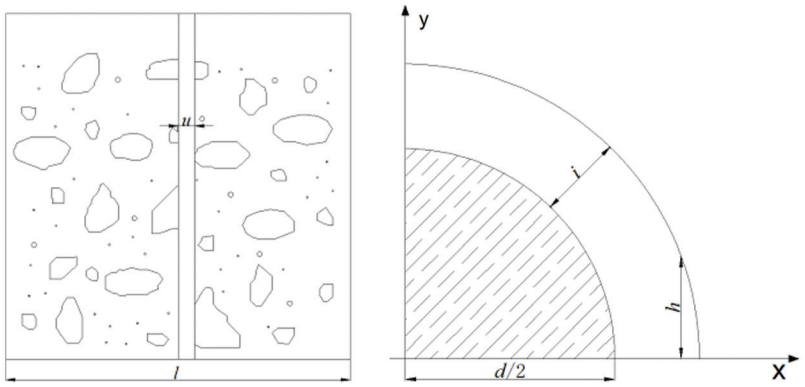

Figure 8: Equivalent film thickness-u and inductive film thickness-h

Based on the assumption of equivalent film thickness, the measured ultrasonic have the relationship as follows:

$$V_d \times l = \mathrm{V}_c(l-u) + \mathrm{V}_p \times u \tag{2}$$

where, V_d is the ultrasonic velocity of modified concrete, km/s; V_c is the ultrasonic velocity of unmodified concrete, km/s; l is the side length of the concrete cube specimen, μm; V_p is the ultrasonic velocity of the modified material in solid state, km/s. Based on the assumption of the inductive film thickness, it is not difficult to draw the following:

$$h_a = \int_{x=0}^{x=d+i} h_x dx \Big/ d_j \tag{3}$$

And,

$$h_x = y_{d+i} - y_d = \sqrt{(\mathrm{d}_j + i)^2 - x^2} - \sqrt{d_j{}^2 - x^2} \quad 0 \le \mathrm{x} \le \mathrm{d}_j + \mathrm{i}; 0 \le \mathrm{y} \le \mathrm{d}_j + i \tag{4}$$

where, h_x is the inductive thickness at x, μm; i is the thickness of the coating, μm; d_j is the diameter of the aggregate, μm; Then the equivalent film thickness–μ(μm) and the inductive film thickness-h_a(μm) should have the following volume equation:

$$ul = 2\pi \sum_{j=1}^{n} \left(\frac{d_j}{2}\right)^2 \times h_a \times k_j \tag{5}$$

k_j is the number of aggregates with a diameter of d_j in a unit volume; Aggregate and cement have the following quality relationships:

$$V_a = \eta \times m_c / \rho_a \tag{6}$$

where, V_a is the total volume of aggregate in the unit volume of concrete, cm³. m_c is the total mass of cement in a unit volume of concrete, g; ρ_a is aggregate density, g/cm³. η is the quality relationship between aggregate and cement. For the total volume of aggregate-V_a:

$$V_a = {}^{4\pi}/_{3} \sum_{j=1}^{j=n} k_j (d_j/2)^3 \tag{7}$$

k_j can be solved by incorporating Eq. (5) into Eq. (6) combining with the aggregate gradation. Solved by Eq. (1) we can get u. Bring u, k_j and Eq. (2) into Eq. (4), i can be solved. Since the aggregate is assumed to be a sphere, $\varnothing = 0.66$ is used for shape conversion. The film thickness corresponding to 4%, 6%, 8% and 10% concentration of PVA is about 29.00 μm, 41.12 μm, 63.82 μm and 98.77 μm respectively using the above method, the calculation results are roughly consistent with the engineering application data.

3.4 Deformation Characteristics

The unconfined compressive stress-strain curve of PA and SA concrete under unconfined uniaxial compression is shown in Fig. 9 (The stress-strain curve of SA10 is not obtained because of the equipment failure).

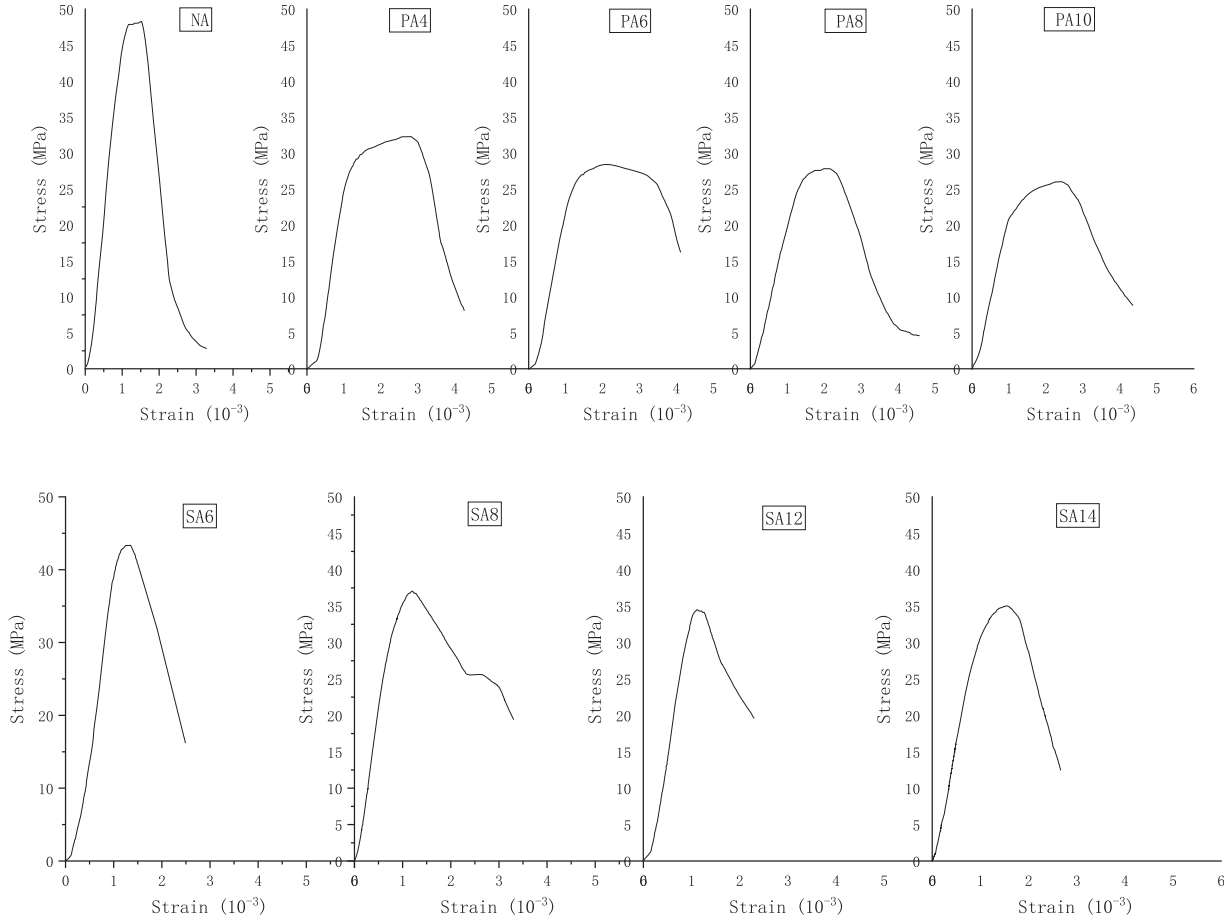

Figure 9: Stress-strain curve of PA and SA concrete

PA-concrete shows obvious plastic deformation. For normal concrete, the cracks between the matrix and the transition zone rapidly expand to make the entire crack system continuous after the concrete stress exceeds 75% of the ultimate load but the deformation of PA-concrete is very slow at this stage. And SA-concrete presents obvious brittle deformation. The chord modulus is used to characterize the elastic modulus [48], and the variation of the elastic modulus and ultimate strain of PA and SA concrete with the concentration is analyzed, as shown in Fig. 10.

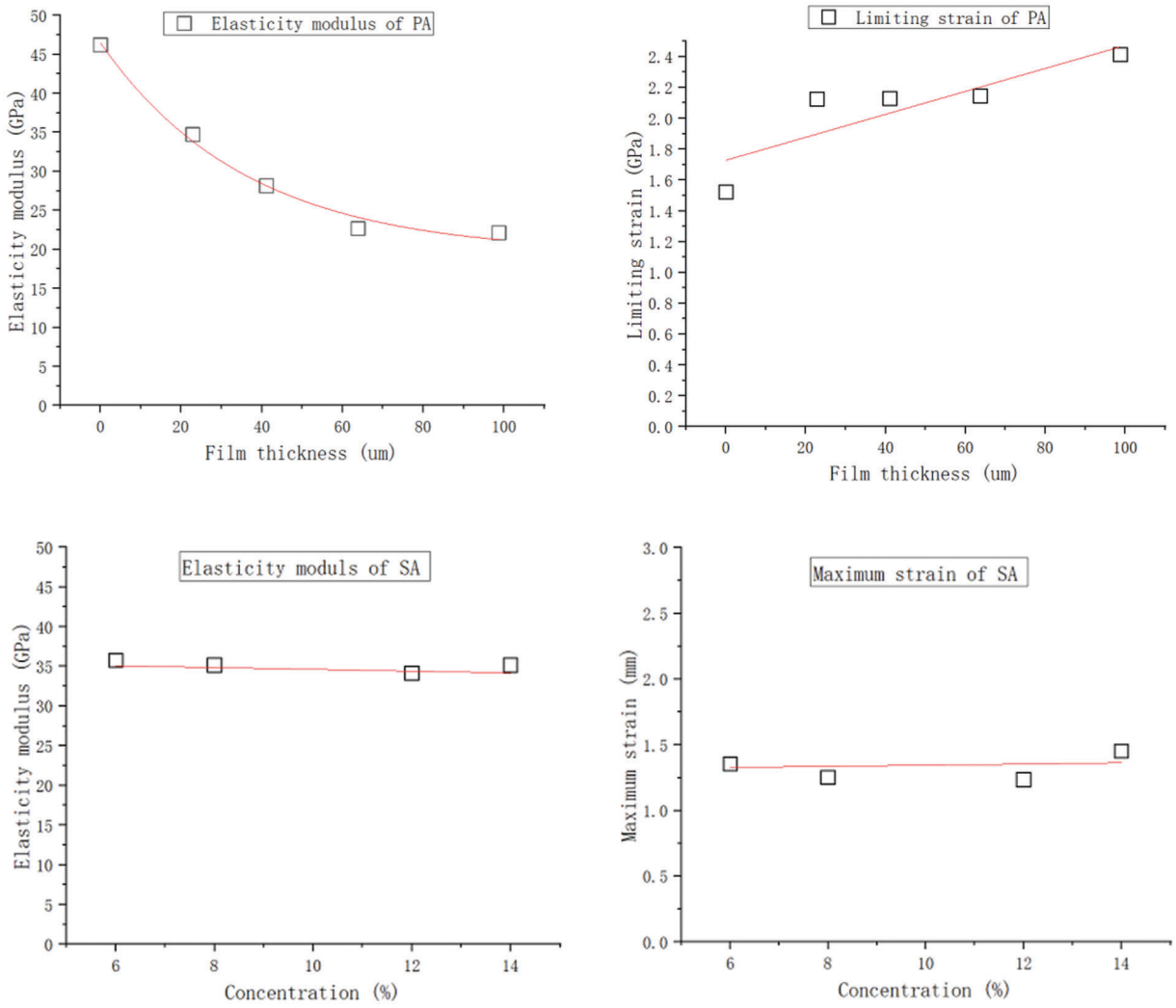

Figure 10: Deformation analysis of PA and SA concrete

The elastic modulus and maximum deformation of PA-concrete decrease and increase respectively with the increase of the concentration. So the PVA has a positive effect on the plastic characteristics of PA-concrete and plastic characteristic has a good correlation with concentration. The elastic modulus and ultimate deformation of SA-concrete do not change significantly with different concentrations, indicating that although the aggregate modification by silane will reduce the compressive strength of the concrete, it has no obvious effect on the stress and strain of the concrete, and all show obvious brittle deformation. The plastic characteristics of PA-concrete and brittle deformation of SA-concrete are also shown in the failure form in Fig. 11.

The fragments do not fall after the PA-concrete is destroyed. P6, PA8, and PA10 concrete show dilatancy. Shear cracks generally form an angle of 20°~30° with the load direction. Traditional plastic concrete is a flexible wall material formed by replacing most of the cement in normal concrete with clay and/or bentonite. Since the elastic modulus of the concrete cut-off wall in the earth dam is very different from that of the foundation, the settlement and displacement of the foundation put a lot of pressure on the top of the cut-off wall and a lot of friction on the side causing the stress is sometimes much higher than the strength of concrete inside of the cut-off wall, and the strain is much higher than the ultimate strain of

concrete causing cracks in the wall and reducing the impermeability. To solve this problem, plastic concrete has appeared. It has a much smaller elastic modulus than common concrete or clay concrete and is similar to the deformation modulus of the surrounding soil, so it can adapt to the deformation of the foundation well and greatly reduce stress in the wall, and prevent cracking [49]. PA concrete shows plastic deformation, so this method can be considered to combine with the method of adding bentonite or clay to increase the plasticity of the matrix while increasing the plasticity of the aggregate to make plastic concrete with stronger crack resistance and this method can also reduce the amount of bentonite. There is no obvious variation in the failure form of SA-concrete. Shear cracks generally form an angle of 20°~30° with the load. After the concrete is destroyed, a large amount of fragments fall and there is no dilatancy.

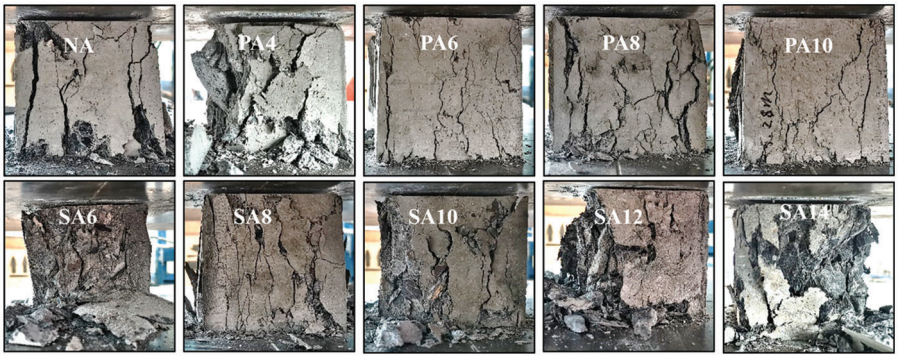

Figure 11: Failure patterns of PA and SA concrete

The strength and strain characteristics of concrete with organic coating aggregate can be estimated reference to the following formulas:

$$\sigma_i = e^{-\Delta i/\omega_1}(\sigma_0 - \omega_2) + \omega_2 \qquad \omega_1 = 28.69 \pm 0.9 \qquad \omega_2 = 23.63 \pm 0.3 \tag{8}$$

$$E_i = e^{-\Delta i/\psi_1}(E_0 - \psi_2) + \psi_2 \qquad \psi_1 = 36.30 \pm 8.0 \qquad \psi_2 = 19.46 \pm 2.0 \tag{9}$$

$$\varepsilon_t = \chi_3 \Delta i + \varepsilon_0 \qquad \chi_3 = 0.0074 \pm 0.0025 \tag{10}$$

where σ is uniaxial compressive strength; Mpa; E is elasticity modulus, GPa; ε is limit deformation, mm.

4 Conclusion

1. Humidity determines the alkali-aggregate reaction. As a hydrophilic waterproof material, PVA can improve the waterproofness of concrete and aggregate significantly, and wrap aggregate well. Concentration will increase the thickness of the PVA film, but it does not improve its waterproofness and hydrotropism. As a hydrophobic waterproof material, silane waterproofing agent can improve the waterproofness of concrete and aggregate significantly too, but it is easy to desquamate from the aggregate during the deformation of the concrete. In terms of water waterproofness, PVA is suit for aggregate and silane is suit for concrete surfaces.

2. PVA coating not only reduces the interfacial adhesion but also reduces frictional resistance of the aggregate surface, and it will improve the ITZ. Aggregate modified concrete by PVA shows obvious plastic deformation and it shows good consistency with film thickness which can be calculated by the ultrasonic velocity of concrete. This paper gives the relationship between plastic properties and film thickness which provides a certain reference for the application of aggregate with organic coating in plastic concrete technology. The aggregate modified by silane waterproofing agent can also reduce the

interfacial adhesion because of the hydrophobicity of the aggregate surface. Its concrete still shows obvious brittle deformation.

Acknowledgement: Thanks to the help provided by Teacher Ai Ting of the Civil Engineering Laboratory of Sichuan University.

Funding Statement: This work was financially supported by the National Natural Science Foundation of China (52108358); China Postdoctoral Science Foundation (2021M693110), and Special Research Associate Project of Chinese Academy of Sciences (E1K2180).

Conflicts of Interest: The authors declare that they have no conflicts of interest to report regarding the present study.

References

1. Li, H. Y. (2007). Environmental prediction model of groundwater contamination in mining area with mine spoils. *International Conference on Mine Hazards Prevention and Control*, pp. 470–475. Qingdao, China.
2. Masoudian, M. S., Zevgolis, I. E., Deliveris, A. V., Marshall, A. M., Heron, C. M. et al. (2019). Stability and characterisation of spoil heaps in European surface lignite mines: A state-of-the-art review in light of new data. *Environmental Earth Sciences, 78(16),* 57. DOI 10.1007/s12665-019-8506-7.
3. Qiao, N., Duan, Y., Wei, X., Shi, X. (2020). Study on landslide monitoring experiment of underground chambers spoil area. *IOP Conference Series Earth and Environmental Science, 456,* 012212. DOI 10.1088/1755-1315/455/1/012212.
4. Chang, L., Mdat, C. (2019). Effect of polypropylene fiber content on the vibration and wind suction resistant performance of alkali-activated slag tunnel fireproof coatings. *Journal of Fuzhou University (Natural Science Edition)*, *47(4),* 527–532. DOI 10.7631/issn.1000-2243.18402.
5. Stanton, T. E. (1940). Expansion of concrete through reaction between cement and aggregate. *Proceedings of the American Society of Civil Engineers, 66(10),* 1781–1811. DOI 10.1061/taceat.0005540.
6. Chang, L., Mdat, C., Jhi, A. (2018). A mechanistic study on mitigation of alkali-silica reaction by fine lightweight aggregates. *Cement and Concrete Research, 104,* 13–24. DOI 10.1016/j.cemconres.2017.10.006.
7. Wang, H., Wu, D., Mei, Z. (2019). Effect of fly ash and limestone powder on inhibiting alkali aggregate reaction of concrete. *Construction and Building Materials, 210(9),* 620–626. DOI 10.1016/j.conbuildmat.2019.03.219.
8. Hudec, P. P., Banahene, N. K. (1993). Chemical treatments and additives for controlling alkali reactivity. *Cement & Concrete Composites, 15(1–2),* 21–26. DOI 10.1016/0958-9465(93)90036-9.
9. Giaccio, G., Celeste Torrijos, M., Milanesi, C., Zerbino, R. (2019). Alkali-silica reaction in plain and fibre concretes in field conditions. *Materials and Structures, 52(2),* 31. DOI 10.1617/s11527-019-1332-2.
10. Grazia, M., Goshayeshi, N., Gorga, R., Sanchez, L., Souza, D. et al. (2021). Comprehensive semi-empirical approach to describe alkali aggregate reaction (AAR) induced expansion in the laboratory. *Journal of Building Engineering, 40,* 102298. DOI 10.1016/j.jobe.2021.102298.
11. Zapała-Sławeta, J., Owsiak, Z. (2018). The use of lithium compounds for inhibiting alkali-aggregate reaction effects in pavement structures. *IOP Conference Series: Materials Science and Engineering, 356,* 12008. DOI 10.1088/1757-899X/356/1/012008.
12. Lya, B., Mp, B., Hs, A., Ma, C., Gdl, D. (2021). Computational modeling of temperature and relative humidity effects on concrete expansion due to alkali-silica reaction. *Cement and Concrete Composites, 124,* 104237. DOI 10.1016/j.cemconcomp.2021.104237.
13. Larive, C. (1998). Apports combines de l'experimentation et de la modelisation a la comprehension de l'alcali-reaction et de ses effets mecaniques. http://www.theses.fr/1997ENPC9707.
14. Merachtsaki, D., Tsardaka, E. C., Anastasiou, E., Zouboulis, A. (2021). Anti-corrosion properties of magnesium oxide/magnesium hydroxide coatings for application on concrete surfaces (sewerage network pipes). *Construction and Building Materials, 312(2),* 125441. DOI 10.1016/j.conbuildmat.2021.125441.

15. Al-Rashed, R., Al-Jabari, M. (2021). Concrete protection by combined hygroscopic and hydrophilic crystallization waterproofing applied to fresh concrete. *Case Studies in Construction Materials, 15(10),* e00635. DOI 10.1016/j.cscm.2021.e00635.
16. Coppola, L. (2021). Protection of concrete structures: Performance analysis of different commercial products and systems. *Materials, 14(13),* 3719. DOI 10.3390/ma14133719.
17. Dm, A., Ect, B., Ea, B., Az, A. (2021). Anti-corrosion properties of magnesium oxide/magnesium hydroxide coatings for application on concrete surfaces (sewerage network pipes). *Construction and Building Materials, 312,* 125441. DOI 10.1016/J.CONBUILDMAT.2021.125441.
18. Kühne, H. (2006). EN 1504-1-10 Products and systems for the protection and repair of concrete structures. https://opus4.kobv.de/opus4-bam/frontdoor/index/index/docId/14525.
19. Dai, J. G., Akira, Y., Wittmann, F. H., Yokota, H., Peng, Z. (2010). Water repellent surface impregnation for extension of service life of reinforced concrete structures in marine environments: The role of cracks. *Cement & Concrete Composites, 32(2),* 101–109. DOI 10.1016/j.cemconcomp.2009.11.001.
20. Bao, J., Li, S., Zhang, P., Xue, S., Ding, Y. (2020). Influence of exposure environments and moisture content on water repellency of surface impregnation of cement-based materials. *Journal of Materials Research and Technology, 9(6),* 12115–12125. DOI 10.1016/j.jmrt.2020.08.046.
21. Felekoglu, B. (2012). A method for improving the early strength of pumice concrete blocks by using alkyl alkoxy silane (AAS). *Construction and Building Materials, 28(1),* 305–310. DOI 10.1016/j.conbuildmat.2011.07.026.
22. Liu, B., Shi, J., Sun, M., He, Z., Tan, J. (2020). Mechanical and permeability properties of polymer-modified concrete using hydrophobic agent. *Journal of Building Engineering, 31(9),* 101337. DOI 10.1016/j.jobe.2020.101337.
23. Poyet, S., Sellier, A., Capra, B., Thevenin-Foray, G., Torrenti, J. M. et al. (2006). Influence of water on alkali-silica reaction: experimental study and numerical simulations. *Journal of Materials in Civil Engineering, 18(4),* 588–596. DOI 10.1061/(ASCE)0899-1561(2006)18:4(588).
24. Merachtsaki, D., Fytianos, G., Papastergiadis, E., Samaras, P., Zouboulis, A. (2020). Properties and performance of novel $Mg(OH)_2$-based coatings for corrosion mitigation in concrete sewer pipes. *Materials, 13(22),* 5291. DOI 10.3390/ma13225291.
25. Shi, Y., Dong, Y., Wang, L., Chen, X., Li, X. (2014). Different chemical composition of aggregate impact on hydraulic concrete interfacial transition zone. *Asian Journal of Chemistry, 26(5),* 1267–1270. DOI 10.14233/ajchem.2014.17203.
26. Wu, K., Han, H., Dong, B. Q., Liu, T. J., de Schutter, G. (2021). Experimental study on concurrent factors influencing the ITZ effect on mass transport in concrete. *Cement and Concrete Composites, 123,* 104215. DOI 10.1016/j.cemconcomp.2021.104215.
27. Pan, Z., Wang, D., Ma, R., Chen, A. (2018). A study on ITZ percolation threshold in mortar with ellipsoidal aggregate particles. *Computers & Concrete, 22(6),* 551–561. DOI 10.12989/cac.2018.22.6.551.
28. Krishnya, S., Elakneswaran, Y., Yoda, Y. Y. (2021). Proposing a three-phase model for predicting the mechanical properties of mortar and concrete. *Materials Today Communications, 29,* 102858. DOI 10.1016/j.mtcomm.2021.102858.
29. Shi, J., Tan, J., Liu, B., Chen, J., He, Z. (2021). Experimental study on full-volume slag alkali-activated mortars: Air-cooled blast furnace slag versus machine-made sand as fine aggregates. *Journal of Hazardous Materials, 403(21),* 123983. DOI 10.1016/j.jhazmat.2020.123983.
30. Shi, J. Y. (2022). Physico-mechanical, thermal properties and durability of foamed geopolymer concrete containing cenospheres. *Construction and Building Materials, 325(1),* 126841. DOI 10.1016/j.conbuildmat.2022.126841.
31. Ahmad, M., Ansari, M. K., Singh, R., Sharma, L. K., Pires, S. (2018). Assessment of potential alkali aggregate reactivity for siliceous and carbonate aggregates: A case study. *Journal of the Geological Society of India, 91(4),* 467–474. DOI 10.1007/s12594-018-0880-3.
32. Magos, I., Balan, C. (2021). Contact angles on spherical hydrophilic surfaces. *12th International Symposium on Advanced Topics in Electrical Engineering (ATEE)*, Bucharest, Romania.
33. Zhang, Y., Zhu, B. (1992). Small angle sessile drop method for low interfacial tension measurement. *Acta Physico-Chimica Sinica, 8(3),* 413–417. DOI 10.3866/PKU.WHXB19920325.

34. Cai, N., Li, Y. X., Cui, D. X. (2014). Application studies on silane hydrophobic agents for concrete protection. *Advanced Materials Research, 1053,* 297–302. DOI 10.4028/www.scientific.net/AMR.1053.297.
35. Barnathunek, D., Widomski, M. K. (2020). Durability of hydrophobic/icephobic coatings in protection of lightweight concrete with waste aggregate. *Materials, 3,* 620. DOI 10.3390/ma14030620.
36. Mehta, P. K., Monteiro, P. (2013). Concrete: Microstructure, properties, and materials. In: *Concrete: Microstructure, properties, and materials*. USA: McGraw-Hill Education.
37. Hallensleben, M. L. (2000). *Polyvinyl compounds, others*. Germany: Wiley VCH Verlag GmbH & Co. KGaA.
38. Williams, P. T. (1983). Proceedings of the seventh international congress on the chemistry of cement, paris 1980, vols. i and iv: Published by Editions Septima, 14 rue Falguière, 75015, Paris, France. *International Journal of Cement Composites & Lightweight Concrete, 5(3),* 213–214. DOI 10.1016/0262-5075(83)90015-5.
39. Ollivier, J. P., Maso, J. C., Bourdette, B. (1995). Interfacial transition zone in concrete. *Advanced Cement Based Materials, 2(1),* 30–38. DOI 10.1016/1065-7355(95)90037-3.
40. Lee, H. J., Michielsen, S. (2006). Technical note-Lotus effect: Superhydrophobicity. *Journal of the Textile Institute, 97(5),* 455–462. DOI 10.1533/joti.2006.0271.
41. Harutyunyan, V. S., Abovyan, E. S., Monteiro, P., Mkrtchyan, V. P., Balyan, M. K. et al. (2003). X-ray diffraction investigations of microstructure of calcium hydroxide crystallites in the interfacial transition zone of concrete. *Journal of the American Ceramic Society, 86(12),* 2162–2166. DOI 10.1111/j.1151-2916.2003.tb03625.x.
42. Maso, J. C. (1996). Interfacial transition zone in concrete. *Advanced Cement Based Materials, 2(1),* 30–38. DOI 10.1016/1065-7355(95)90037-3.
43. Shukla, S. K. (2013). *Rock mechanics*. USA: CRC Press.
44. Malhotra, V. M., Carino, N. J. (2004). Handbook on nondestructive testing of concrete. In: *Handbook on nondestructive testing of concrete*. UK: Taylor & Francis Group.
45. Robins, P. J. (1980). The point-load strength test for concrete cores. *Magazine of Concrete Research, 32(111),* 101–111. DOI 10.1680/macr.1980.32.111.101.
46. Gora, J., Piasta, W. (2020). Impact of mechanical resistance of aggregate on properties of concrete. *Case Studies in Construction Materials, 13(5),* e00438. DOI 10.1016/j.cscm.2020.e00438.
47. Sonnenberg, A., Al-Mahaidi, R., Taplin, G. (2003). Behaviour of concrete under shear and normal stresses. *Magazine of Concrete Research, 55(4),* 367–372. DOI 10.1680/macr.2003.55.4.367.
48. Hou, H., Zhao, G., Chen, L., Li, H. (2021). Springback behavior and a new chord modulus model of copper alloy during severe plastic compressive deformation. *Journal of Materials Processing Technology, 290(5−6),* 116974. DOI 10.1016/j.jmatprotec.2020.116974.
49. Herrmann, H., Bucksch, H. (2014). Plastic concrete wall. In: *Dictionary geotechnical engineering/Wörterbuch geoTechnik*. Germany: Springer.